Hot recombination of photogenerated ion pairs

Gladkikh, Vladislav; Burshtein, Anatoly I.; Feskov, Serguei V.; Ivanov, Anatoly I.; Vauthey, Eric

Hot recombination of photogenerated ion pairs

Vladislav Gladkikh and Anatoly I. Burshtein[a)]
Weizmann Institute of Science, Rehovot 76100, Israel

Serguei V. Feskov and Anatoly I. Ivanov[b)]
Department of Physics, Volgograd State University, University Avenue 100, Volgograd 400062, Russia

Eric Vauthey[c)]
Department of Physical Chemistry, University of Geneva, 1211 Geneva, Switzerland

(Received 7 July 2005; accepted 27 October 2005; published online 30 December 2005)

The recombination dynamics of ion pairs generated upon electron transfer quenching of perylene in the first singlet excited state by tetracyanoethylene in acetonitrile is quantitatively described by the extended unified theory of photoionization/recombination. The extension incorporates the hot recombination of the ion pair passing through the level-crossing point during its diffusive motion along the reaction coordinate down to the equilibrium state. The ultrafast hot recombination vastly reduces the yield of equilibrated ion pairs subjected to subsequent thermal charge recombination and separation into free ions. The relatively successful fit of the theory to the experimentally measured kinetics of ion accumulation/recombination and free ion yield represents a firm justification of hot recombination of about 90% of primary generated ion pairs. © *2005 American Institute of Physics*. [DOI: 10.1063/1.2140279]

I. INTRODUCTION

Most theories of electron transfer reactions in condensed media, reviewed in Refs. 1,2, incorporate as input data the thermal transfer rates between reactants separated by a distance r. These rates are controlled either by the tunneling near the intersection point of reactant and product levels or the system delivery to this point from the equilibrium position. It is usually assumed that the system motion along the reaction coordinate q proceeds faster than the modulation of the interparticle distance r by encounter diffusion and that the transfer always starts from the equilibrium position in the reactant well. If one of these conditions is violated, the encounter theory has to account for the occurrence of the process along $\mathbf{r}$ and q simultaneously. This has been done once for a diffusion-controlled thermal ionization competing with the diffusion along the reaction coordinate.[3] In the present work, we consider the geminate recombination of ion pairs produced by bimolecular photoinduced electron transfer (ionization). The backward electron transfer proceeding before thermalization, known as "hot recombination," does not need any thermal activation and is therefore more efficient and much faster than the subsequent thermal recombination that conventional theories are confined to.

The chemical system investigated here consists of perylene (Pe) in the first singlet excited state as electron donor in the presence of tetracyanoethylene (TCNE) in acetonitrile. The fluorescence quenching dynamics of Pe after excitation by an ultrashort optical pulse was recently studied both experimentally and theoretically.[4] It was concluded that the electron transfer quenching results to both the ground and the excited state of the ion pair with the rates W and W^*, respectively,

$$\mathrm{Pe^+TCNE^-} \overset{W_I}{\leftarrow} \mathrm{Pe^*} + \mathrm{TCNE} \overset{W_I^*}{\rightarrow} \mathrm{Pe^{+*}TCNE^-}.$$

Using the abbreviations, D for Pe and A for TCNE, we consider a four-level energy scheme (Fig. 1) including vibrational sublevels ($n=0, 1, 2, \ldots$) of the DA and D^+A^- states. According to this scheme, both the excited and the ground channels of ionization-recombination include hot transitions. These two ionization channels are depicted separately in Fig. 2. It is useful to introduce the probabilities α and α^* to produce equilibrated ion pairs through the ground and the excited channels, respectively. These pairs recombine thermally to the neutral ground state.

The overall reaction scheme includes the recombination of charged products assisted by vibrational and solvent relaxation. After the forward electron transfer generating the ion pair in the ground state, the population moves down diffusively and crosses a number of vibronic sublevels of neutral products before reaching the equilibrium. A fraction $1-\alpha$ of the ion-pair population recombines during this stage, i.e., prior to thermalization, which is approximately equal to the time scale of the longitudinal solvent relaxation τ_L. The remaining fraction of the ion-pair population (α) reaches equilibrium and recombines thermally with a rate W_R [see Figs. 1 and 2]. The fate of the excited ion-pair population is more complex [see Fig. 2]. These ion pairs are born near contact,[4] at a distance where electron transfer (either forward or backward) is essentially limited by the solvent relaxation ($1/\tau_L$). These ion pairs undergo charge recombination to one of the vibrational states of the neutral products (dotted levels in Fig. 1) with approximately this rate. This is followed by the

[a)]Electronic mail: cfbursh@wisemail.weizmann.ac.il
[b)]Electronic mail: physic@vlink.ru
[c)]Electronic mail: eric.vauthey@chiphy.unige.ch

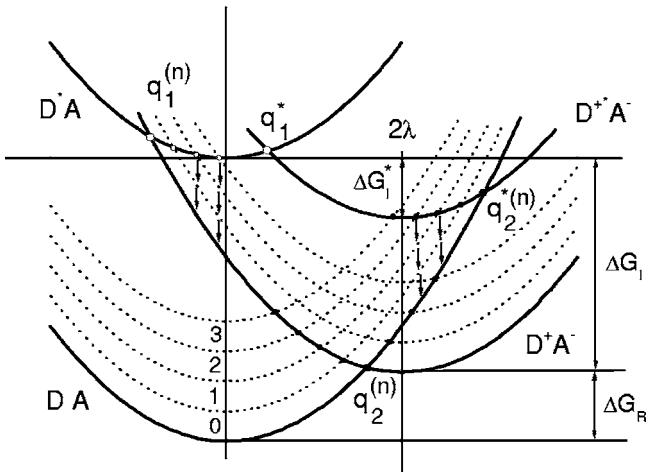

FIG. 1. Ground and excited electronic states of the reactants, DA and D^*A, and charged products, D^+A^- and $D^{+*}A^-$, at contact distance. The dotted lines represent vibrational excited states ($n=1, 2, 3$); the crossing points for forward transfer are marked by circles (○) and for backward transfer by bullets (•). The arrows show the direction of the intramolecular vibrational relaxation.

even faster intramolecular vibrational relaxation to the neutral ground state. Afterwards, this neutral population passes diffusively through the lowest crossing point with the charge-transfer states where a fraction α^* converts back to the ion pair in the ground state. This ion-pair population undergoes equilibration and thermal recombination with a rate W_R. Therefore, the equilibrated ion-pair population, which recombines thermally, consists of the fractions α and α^* of the primary ion-pair populations generated by the parallel pathways [(A) and (B) in Fig. 2], with hot recombination taking place earlier.

The dynamics of hot-electron transfer at a fixed interparticle distance has been extensively studied with the nonequilibrium generalization of the golden rule formula.[5,6] As the transfer was assumed to be limited by weak electronic coupling, the hot transfer yield was very small. In the limit of weak transfer, almost all the neutral ground-state population originating from the recombination of excited ion pairs undergoes complete equilibration, i.e., $\alpha^* \ll 1$. Similarly, the hot charge recombination of the ion pairs formed in the ground state D^+A^- is almost insignificant, i.e., $\alpha \approx 1$. As a result, this equilibrated ion-pair population is the product of forward electron transfer with the rate W_I and should represent 89%–96% of the total quenching product. However, the opposite result was found experimentally:[7] Only 10% of the quenching product ends up as equilibrated ion pairs. This indicates that hot recombination is efficient and should thus be better described with a stochastic approach[8,9] than with perturbation theory. When the reaction is limited by the diffusion to the crossing point rather than by the electronic coupling, this approach allows $\alpha \ll 1$ to be obtained. This is the so-called dynamic solvent effect (DSE) regime realizing at the highest friction. It was first studied in the Marcus normal region[8,10–15] and opposed to the other regimes (of moderate and low friction) in a few reviews.[16,17] Later on the same analysis was done also for the Marcus inverted region where DSE takes place as well.[18]

The simplest version of a stochastic theory accounting for the DSE was first developed in Ref. 19. It neglects the reversibility of the transfer in the crossing point, because of the instantaneous decay of the transfer product and thus reduces the problem to a single level with a sink. A similar approach to the problem was applied in Ref. 20 and then in Ref. 21. There is, however, no necessity for such a simplification. Using the most general stochastic approach to the problem, the reversible transfer between three intersecting levels, D^*A, D^+A^-, and DA, has been studied in Ref. 22. The arrangement of the energy levels in the case E of Fig. 4(a) in Ref. 22 is exactly the same as in Fig. 1. In the case of fast transfer, the kinetics of ion-pair decay consists of a fast hot recombination and a subsequent much slower thermal recombination.[22] Perturbation theory holds only in the opposite limit of the weak transfer where the hot stage is almost eliminated [Fig. 4(b) of the same work]. The relationship between stochastic and perturbation theories has been investigated in more detail in Ref. 23. In this work, the analytically estimated α value was shown to change from 0 to 1 when the transfer in the intersection point becomes more efficient.

In the following, only the results of the last two papers[22,23] will be used. They will be incorporated in the unified theory (UT) of irreversible photoionization and recombination, which accounts for the r dependence of all electron transfer rates and the encounter diffusion of the counterions in a Coulomb well.[1] As the original UT (Refs. 24,25) deals with thermal electron transfer only, it will be generalized to account for hot recombination prior to equilibration.

II. EXTENDED UNIFIED THEORY

Using a general approach, we consider a set of energy levels accounting for the electronic states and their vibra-

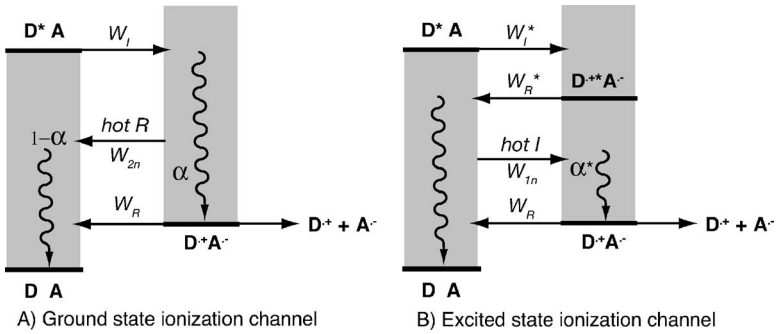

FIG. 2. Energy-level schemes illustrating the two channels to the thermalized ion pairs. The grey areas stand for the nonthermalized levels while the wavy arrows represent vibrational and/or solvent relaxation.

tional sublevels[26] involved in the overall reaction scheme [Figs. 2]. All energies are assumed to have a quadratic dependence on the solvent coordinate q,

$$U_{D^*A} = \frac{q^2}{4\lambda}, \quad U^{(n)}_{D^+A^-} = \frac{(q-2\lambda)^2}{4\lambda} + \Delta G_I + n\hbar\Omega,$$

$$U_{D^{+*}A^-} = \frac{(q-2\lambda)^2}{4\lambda} + \Delta G^*_I, \tag{1}$$

$$U^{(n)}_{DA} = \frac{q^2}{4\lambda} + \Delta G_I + \Delta G_R + n\hbar\Omega,$$

where $\Delta G_I < 0$ and $\Delta G_R < 0$ are the free energies of the primary ionization and of the subsequent charge recombination to the ground state, respectively, ΔG^*_I is the free energy of electron transfer to the excited ion pair (Fig. 1), λ is the solvent reorganization energy, Ω is the frequency of intramolecular vibrational mode, and $\hbar$ is the Planck constant. The index n stands for the nth vibrational sublevel of the appropriate electronic state.

As the relaxation of the high-frequency modes of the excited reactant is assumed to be much faster than all the electron transfer reactions considered, and as $\hbar\Omega \gg k_B T$, the vibrational excited states are not included in U_{D^*A}. Moreover, since the transition between U_{D^*A} and $U_{D^{+*}A^-}$ proceeds in the Marcus normal region, the vibrational excited sublevels of the latter are not considered as well.

The reaction scheme [Figs. 2] shows the two pathways associated with the forward electron transfer to the ion-pair ground state D^+A^- and to the ion pair in the excited state $D^{+*}A^-$. These processes occur at the term crossing points $q^{(n)}_1$ and q^*_1, where $U_{D^*A}(q^{(n)}_1) = U^{(n)}_{D^+A^-}(q^{(n)}_1)$ and $U_{D^*A}(q^*_1) = U_{D^{+*}A^-}(q^*_1)$ (Fig. 1), that is, at

$$q^{(n)}_1 = \lambda + \Delta G_I + n\hbar\Omega, \quad q^*_1 = \lambda + \Delta G^*_I. \tag{2}$$

Similarly, charge recombination from the ground and excited ion states takes place at the crossing points $q^{(n)}_2$ and $q^{*(n)}_2$ (Fig. 1), where the energies of the D^+A^- and $D^{+*}A^-$ states are equal to those of the DA state, respectively, that is, at

$$q^{(n)}_2 = \lambda - \Delta G_R - n\hbar\Omega,$$
$$q^{*(n)}_2 = \lambda + \Delta G^*_I - \Delta G_I - \Delta G_R - n\hbar\Omega. \tag{3}$$

It is also seen from Fig. 1 that the crossing points $q^{(n)}_2$ lie to both the left and the right of $q^{(0)}_2$, so the index n in the equation for $q^{(n)}_2$ may be either positive or negative.

The positions of all crossing points depend implicitly on r because

$$\lambda(r) = \lambda_0(2 - \sigma/r) \tag{4}$$

depends on the inter-reactant distance. In acetonitrile the contact reorganization energy is taken as

$$\lambda_0 = 1.15 \text{ eV}, \tag{5}$$

and the average contact distance between Pe and TCNE is $\sigma = 5$ Å.[4]

The bimolecular forward electron transfer (ionization) is universally described by the differential encounter theory (DET) equations,[1,24,25]

$$\dot{N} = -ck_I(t)N(t) - N(t)/\tau_D, \tag{6}$$

where $c = [A] = \text{const}$ and $N(t) = [D^*]$ is the survival probability of the excited donor, provided that initially $N(0) = 1$, $k_I(t)$ is the time-dependent rate constant of ionization, and τ_D is the lifetime of the excited donor in the absence of quencher.

In the original formulation of DET, $k_I(t)$ is the average product of the thermal ionization rate $W_I(r)$ and the pair distribution function of the reactants $n(r,t)$.[1] To account for dynamic solvent effects, we extend the coordinate space to include the solvent coordinate q as follows.[3]

$$k_I(t) = \int w_I(r,q)\nu(r,q,t)dq\, d^3r, \tag{7}$$

where w_I is the r- and q-dependent rate of ionization and $\nu(r,q,t)$ is the distribution function of the D^*A pairs in the extended coordinate space. The latter obeys the following equation:[3]

$$\frac{\partial \nu(r,q,t)}{\partial t} = -w_I(r,q)\nu(r,q,t) + (\hat{\mathbf{D}} + \hat{\mathbf{L}})\nu(r,q,t), \tag{8}$$

where the operator of encounter diffusion of the neutral reactants is

$$\hat{\mathbf{D}} = \frac{D}{r^2}\frac{\partial}{\partial r}r^2\frac{\partial}{\partial r}, \tag{9}$$

D being the encounter diffusion coefficient, and

$$\hat{\mathbf{L}} = \frac{1}{\tau_L}\left[1 + q\frac{\partial}{\partial q} + 2\lambda k_B T\frac{\partial^2}{\partial q^2}\right] \tag{10}$$

is the diffusion operator in the solvent coordinate q. τ_L is the longitudinal dielectric relaxation time of the solvent.

Since there are several parallel channels of ionization at the points $q^{(n)}_1$ and q^*_1, the total rate $w_I(r,q)$ is

$$w_I(r,q) = \sum_n w^{(n)}_I(r,q) + w^*_I(r,q)$$
$$= \sum_n \frac{2\pi V^2_{In}(r)}{\hbar}\delta(q - q^{(n)}_1(r))$$
$$+ \frac{2\pi V^{*2}_I(r)}{\hbar}\delta(q - q^*_1(r)), \tag{11}$$

where $V_I(r)$ and $V^*_I(r)$ are the electronic coupling constants between the D^*A and D^+A^- states and between the D^*A and $D^{+*}A^-$ states, respectively. The quantity $V^2_{In}(r)$ includes the Franck-Condon factor for the vibrational transition $0 \to n$,

$$V^2_{In}(r) = V^2_I(r)\frac{e^{-S_I}S^n_I}{n!}, \tag{12}$$

where $S_I = \lambda_{iI}/\hbar\Omega$, λ_{iI} being the reorganization energy of intramolecular vibrational mode for the electron transfer processes from D^*A. The electronic coupling constants $V_I(r)$

and $V_I^*(r)$ are assumed to decrease exponentially in r space with the characteristic decay length L_I,

$$V_I(r) = V_I e^{-(r-\sigma)/L_I}, \quad V_I^*(r) = V_I^* e^{-(r-\sigma)/L_I}. \tag{13}$$

The accumulation and decay of the ion pairs produced by ionization can be studied within UT (Ref. 1) after its proper generalization. We first introduce the distribution functions in the extended coordinate space $\mu(r,q,t)$ and $\mu^*(r,q,t)$ for the ion pairs in the ground and excited states, and $\pi(r,q,t)$ for the neutral pairs in the ground state DA. The time evolution of these functions obeys the following diffusion equations:

$$\frac{\partial \mu}{\partial t} = \sum_n w_I^{(n)} N(t)\nu + \sum_{n\leqslant 0} w_R^{(n)}\pi - \sum_{n\geqslant 0} w_R^{(n)}\mu + (\hat{\mathbf{D}}_{\mathbf{cs}} + \hat{\mathbf{L}}_{\mathbf{cs}})\mu, \tag{14a}$$

$$\frac{\partial \mu^*}{\partial t} = w_I^* N(t)\nu + w_R^{*(0)}\pi - \sum_{n\geqslant 0} w_R^{*(n)}\mu^* + (\hat{\mathbf{D}}_{\mathbf{cs}} + \hat{\mathbf{L}}_{\mathbf{cs}})\mu^*, \tag{14b}$$

$$\frac{\partial \pi}{\partial t} = -w_R^{*(0)}\pi + \sum_{n\geqslant 0} w_R^{(n)}\mu - \sum_{n\leqslant 0} w_R^{(n)}\pi + \sum_{n\geqslant 0} w_R^{*(n)}\mu^* + (\hat{\mathbf{D}} + \hat{\mathbf{L}})\pi, \tag{14c}$$

with

$$\hat{\mathbf{D}}_{\mathbf{cs}} = \frac{D}{r^2}\frac{\partial}{\partial r} r^2 e^{-U_c/k_B T}\frac{\partial}{\partial r} e^{U_c/k_B T}, \tag{15}$$

$$\hat{\mathbf{L}}_{\mathbf{cs}} = \frac{1}{\tau_L}\left[1 + (q-2\lambda)\frac{\partial}{\partial q} + 2\lambda k_B T \frac{\partial^2}{\partial q^2}\right], \tag{16}$$

where $U_c(r) = -e^2/\varepsilon(r)r$ is the Coulomb potential accounting for the spatial dispersion of the dielectric constant.

In Eqs. (14), the recombination rates $w_R^{(n)}(r,q)$ and $w_R^{*(n)}(r,q)$ through the ground and excited channels are

$$w_R^{(n)} = \frac{2\pi V_{Rn}^2(r)}{\hbar}\delta(q - q_2^{(n)}(r)), \tag{17}$$

$$w_R^{*(n)} = \frac{2\pi V_{Rn}^{*2}(r)}{\hbar}\delta(q - q_2^{*(n)}(r)), \tag{18}$$

with

$$V_{Rn}^2(r) = V_R^2(r)\frac{e^{-S_R}S_R^n}{n!}, \tag{19}$$

where $S_R = \lambda_{iR}/\hbar\Omega$, λ_{iR} being the reorganization energy of the intramolecular vibrational modes for the charge recombination processes to the neutral ground state. The r dependencies of the electronic coupling constant for charge recombination are

$$V_R(r) = V_R e^{-(r-\sigma)/L_R}, \quad V_R^*(r) = V_R^* e^{-(r-\sigma)/L_R}. \tag{20}$$

Equations (8) and (14) should fulfill the boundary conditions[1]

$$\left.\frac{\partial \nu(r,q,t)}{\partial r}\right|_{r=\sigma} = 0, \quad \lim_{q\to\pm\infty}\nu(r,q,t) = 0, \tag{21a}$$

$$\left.\frac{\partial \mu(r,q,t)}{\partial r}\right|_{r=\sigma} = 0, \quad \lim_{q\to\pm\infty}\mu(r,q,t) = 0, \tag{21b}$$

$$\left.\frac{\partial \mu^*(r,q,t)}{\partial r}\right|_{r=\sigma} = 0, \quad \lim_{q\to\pm\infty}\mu^*(r,q,t) = 0, \tag{21c}$$

$$\left.\frac{\partial \pi(r,q,t)}{\partial r}\right|_{r=\sigma} = 0, \quad \lim_{q\to\pm\infty}\pi(r,q,t) = 0, \tag{21d}$$

and the initial conditions

$$\nu(r,q,0) = \varphi_1(q) = (4\pi\lambda T)^{-1/2}\exp(-q^2/4\lambda T), \tag{22}$$

$$\mu(r,q,0) = \mu^*(r,q,0) = \pi(r,q,0) = 0. \tag{23}$$

The total amount of ion pairs surviving at time t is calculated as a sum

$$P_t(t) = P(t) + P^*(t), \tag{24}$$

where

$$P(t) = c\int d^3r \int \mu(r,q,t)dq,$$

$$P^*(t) = c\int d^3r \int \mu^*(r,q,t)dq \tag{25}$$

are the populations of the ground and excited ion pairs, respectively.

It is also useful to introduce the r distributions of D^+A^- and $D^{+*}A^-$ pairs initially produced through the ground- and the excited-state channels $m(r)$ and $m^*(r)$,

$$m(r) = \int_0^\infty dt\, N(t)\int dq \sum_n w_I^{(n)}(r,q)\nu(r,q,t), \tag{26a}$$

$$m^*(r) = \int_0^\infty dt\, N(t)\int dq\, w_I^*(r,q)\nu(r,q,t), \tag{26b}$$

where $\nu(r,q,t)$ and $N(t)$ obey Eqs. (6) and (8).

Equations (6)–(24) provide a formal basis for the theory of ionization and geminate recombination accounting explicitly for hot transitions. This model was investigated numerically using a simulation algorithm given in the Appendix. The results of the simulation are presented in the next section.

III. REPRODUCING THE KINETICS OF QUENCHING AND CHARGE RECOMBINATION

Two independent sets of experimental data have to be reproduced: (1) the time dependence of the excited-state population $N(t)$ and (2) the time dependence of the ground-state-ion pair population $P(t)$.[7] Since the parameters for charge recombination do not affect the ionization dynamics in Eq. (8), we will follow Ref. 4 and start with the fitting of $N(t)$. Below we present the results for $c = 0.32\ M$ only, though analogous results are obtained for $c = 0.16\ M$ as well.

The following fixed parameters were used:[4] $\Delta G_I = -2.14$ eV, $\Delta G_I^* = -0.6$ eV, $\Delta G_R = -0.69$ eV, $\Omega = 0.1$ eV, $L_I = 1.24$ Å, and $\tau_D = 4.34$ ns. On the other hand, the parameters V_I, V_I^*, S_I, and D were adjusted.

A remark concerning the choice of the solvent relaxation time τ_L should be added. Like the other solvents, acetonitrile exhibits non-Markovian polarization relaxation dynamics, which is usually described in terms of several solvent modes with different relaxation times. Acetonitrile is characterized by at least two modes with an ultrafast inertial mode having a relaxation time $\tau_1 \approx 0.2$ ps and a slower Debye-type mode with $\tau_2 \approx 0.5$ ps.[27] Only the latter mode was taken into account because, with the energetic parameters adopted here, the hot transitions predominantly occur when the relaxation of the fastest mode is over and before the slowest mode has started. Of course, the Markovian approach used in this paper can only yield a limited precision of the description.

The strategy for choosing the best-fit parameters was the following. In the ionization kinetics, several regimes, which are controlled by different parameters, can be distinguished. The quenching at early time proceeds at the kinetic regime and can be well described with a rate constant $k_0 = k_I(t=0)$.[4] At this stage, the initial equilibrium distribution of reactants in both q and r spaces is assumed not to be perturbed. This quantity can be calculated using Eq. (7) with $\nu(r,q,0)$ determined by Eq. (22). Its value $k_0 = 322.6$ Å^3/ps was found earlier from the best fit of the short-time kinetics in the 0–6.5 ps interval.[4] The V_I, V_I^*, and S_I parameters able to reproduce this k_0 value were then chosen. This allowed the reduction of the number of independent parameters. At longer times, the quenching is controlled by the diffusive delivery of the reactants to the ionization zone. In this regime, the role of D is dominant, and its value can be determined rather precisely from the analysis of the dynamics of the excited-state population $N(t)$ in the 0.2–1.2 ns interval (see Fig. 3 of Ref. 4). The excited-state population dynamics measured in an intermediate time interval (1–300 ps) was used for the determination of the other parameters.

A. Double-channel ionization model

A few sets of parameters, which can be considered as candidates for the best fit of quenching kinetics, were found. At least two of them reproduce the experimental data of Ref. 4 quite well.

The first set of parameters is the same as that found in Ref. 4 within the framework of the DET. These parameters are

$$V_I = 0.123 \text{ eV}, \quad V_I^* = 0.138 \text{ eV}, \quad S_I = 0, \quad D = 3.05 \times 10^{-5} \text{ cm}^2/\text{s}. \tag{27}$$

Figure 3(a) shows that the excited-state dynamics $N(t)$, calculated earlier in Ref. 4, can be well reproduced with these parameters.

This close agreement between our results and those obtained within the original DET is not surprising. Because ionization through the ground channel occurs in the far Marcus inverted region, the ion pairs should be predominantly formed at relatively large inter-ionic distances. This is illustrated by the $m(r)$ dependence shown in Fig. 4(a). Since the electronic coupling at such distances is very weak, ionization proceeds mostly as a nonadiabatic reaction and does not violate the thermal distribution over the reaction coordinate q.

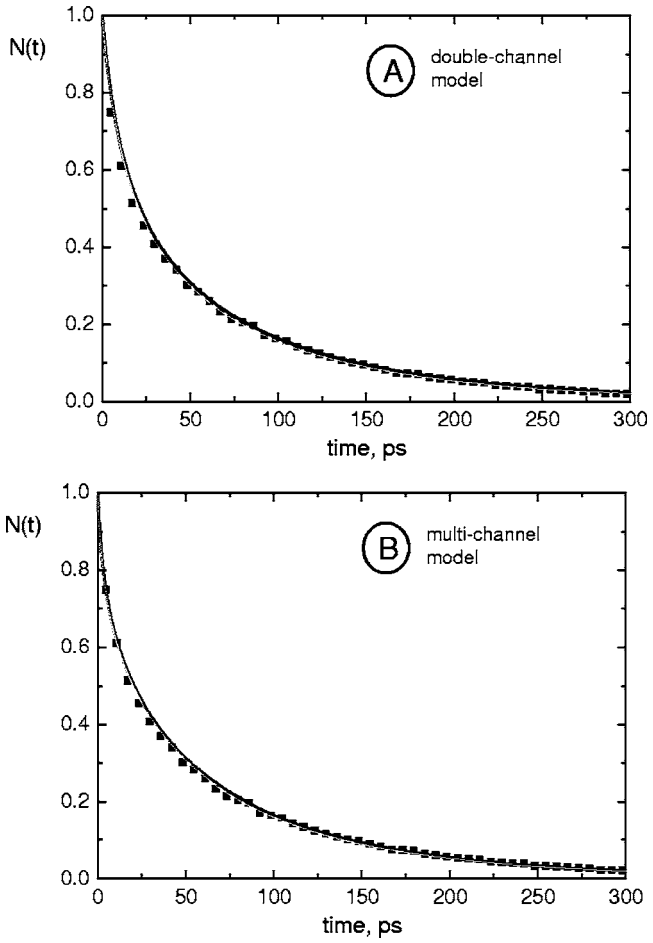

FIG. 3. Best fit of the ionization kinetics at $c = 0.32M$ and reported in Ref. 7 (dots) using the double-channel model (A) and the multichannel model (B). The best-fit parameters are given by Eqs. (27) and (28), respectively.

B. Multichannel ionization model

A rather good fit of the ionization kinetics $N(t)$ to the experimental data [see Fig. 3(b)] was achieved with the following parameters:

$$V_I = 0.048 \text{ eV}, \quad V_I^* = 0.057 \text{ eV}, \quad S_I = 2, \quad D = 3.95 \times 10^{-5} \text{ cm}^2/\text{s}. \tag{28}$$

Since $S_I = 2$, the forward electron transfer proceeds through several vibrational channels at $q_1^{(n)}$. This changes considerably the energetics of ionization and decreases the electronic coupling constants V_I and V_I^*. The vibrational sublevels lower the effective activation barrier of ionization, shifting the reaction closer to the contact distance $r = \sigma$. The distance distribution of the ion pairs produced by ionization is presented in Fig. 4(b). In this case, a somewhat larger value of the diffusion coefficient D was used to reproduce the observed dynamics at long time scale.

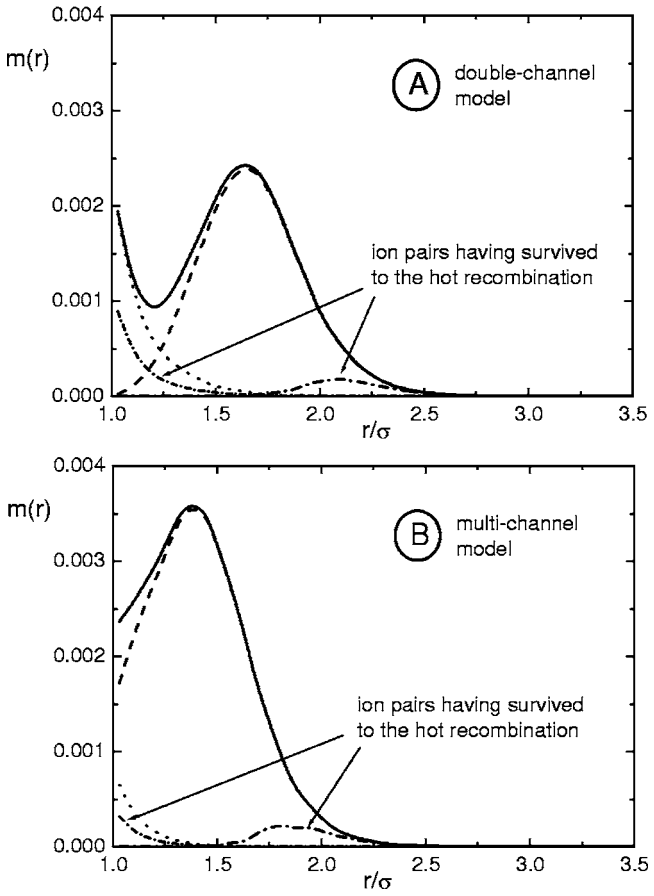

FIG. 4. Distributions of ion pairs generated in the ground state D^+A^- (dashed lines) and the excited state $D^{+*}A^-$ (dotted lines) as a function of the separation distance $m(r)$ and $m^*(r)$: (A) double-channel model with parameters given by Eq. (27) and (B) multichannel model [Eq. (28)]. The solid lines are the overall ion-pair distributions.

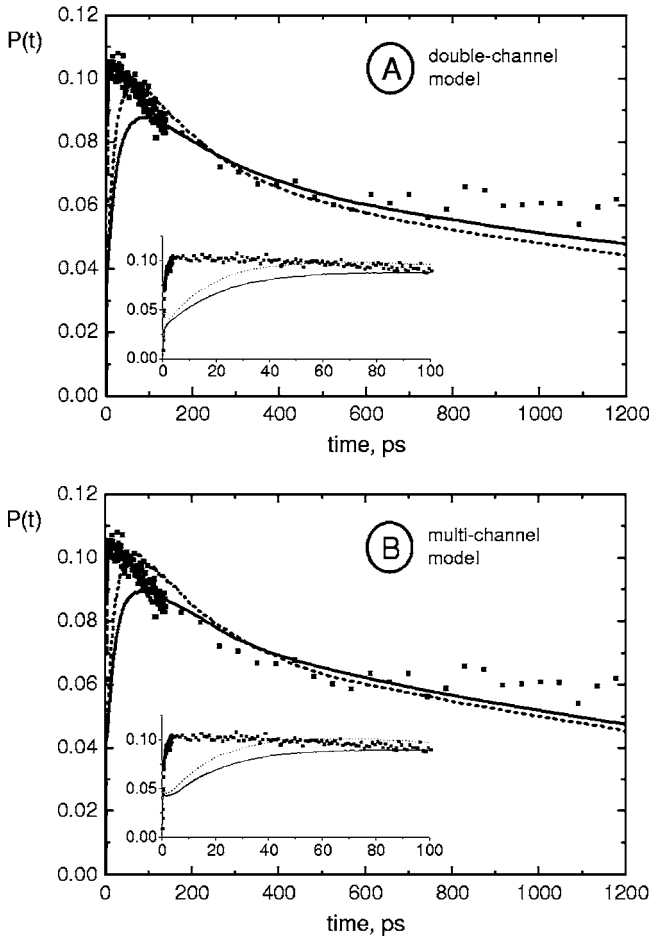

FIG. 5. Best fit of the ion-pair accumulation/recombination kinetics measured with $c=0.32M$ and reported in Ref. 7 (dots) using the double-channel model (A) and the multichannel model (B). The solid lines are the numerical results obtained within the original model [parameters of the fits are given by Eqs. (29) and (30)], while the dashed lines are the same results but accounting for $D(r)$ and $\epsilon(r)$ dependencies with $\Lambda=1.6$ Å ($V_R=V_R^*=0.15$ eV, for the double-channel model, and $V_R=V_R^*=0.075$ eV for the multichannel model).

One remark concerning the sensitivity of the numerical curve $N(t)$ to a particular choice of the fitting parameters needs to be added. Since the efficiency of the excited-state ionization channel is considerably lower than that of the ground-state one, the ionization kinetics is weakly sensitive to the magnitude of V_I^*, and therefore the uncertainty on this value obtained from the fit is rather large. On the other hand, a variation of the other fitting parameters within 5% leads to a noticeable degradation of the fit.

C. Ion-pair accumulation-recombination kinetics

For the fitting of the ion-pair kinetics $P(t)$ to the experimental data, the best-fit parameters in Eq. (27) or alternatively in Eq. (28) were used as input data and only the quantities V_R, V_R^*, L_R, and S_R were adjusted.

With the parameters from Eq. (27), a rather good fit of $P(t)$ to the experimental data in the 80–500 ps time window was achieved [Fig. 5(a)]. It shows that the equilibrated ion-pair population never exceeds 11% of the primary quenching product population $P_t(t)$. The reason is that most of the initially produced ion-pair population undergo ultrafast hot recombination after their birth at the q_1 point. This conclusion will be confirmed in the next section by the direct estimation of hot transition probability.

The free ion yield $P(\infty)$ measured independently by photoconductivity is even smaller and amounts to 6%.[7] This number was used to relate the experimental time profiles of the transient absorption, given in the same work in arbitrary units, to the absolute ion yield. A good fit of the double-channel model [Eq. (27)] at long times was obtained with the following set of parameters:

$$V_R = 0.165 \text{ eV}, \quad V_R^* = 0.165 \text{ eV}, \quad S_R = 3, \quad L_R = 2.2 \text{ Å}. \tag{29}$$

These values are in relatively good agreement with those found in the literature. In particular, the contact values of the electronic coupling constant V_R and V_R^* are comparable with those found in a few independent studies on exciplexes (contact ion pairs). Values between 0.11 and 0.13 eV and between 0.15 and 0.4 eV are reported in Refs. 28 and 29, respectively.

The fit of the multichannel model to the ion-pair kinetics $P(t)$ using the ionization parameters given in Eq. (28) is presented in Fig. 5(b). The best fit was obtained with the following set of parameters:

$$V_R = 0.093 \text{ eV}, \quad V_R^* = 0.093 \text{ eV}, \quad S_R = 3, \quad L_R = 2.2 \text{ Å}. \tag{30}$$

Since the ion pairs are produced at closer distance than in the double-channel model, efficient hot recombination can be achieved with smaller electronic coupling constants V_R and V_R^*.

It should be noted that the recombination dynamics at relatively short times $t<80$ ps could not be reproduced. However, a rather good fit was obtained at moderate times 80 ps$<t<500$ ps. Finally, the simulations at long times $t>500$ ps predict a slow decay of the ion-pair population due to the diffusion-assisted geminate recombination, while the experimentally observed population remains constant.

The ion-pair population dynamics is determined by the competition between production and recombination. The discrepancy at short times can be due to either an underestimation of the ion production or an overestimation of the ion recombination.

The approach used here is only applicable if the electronic transitions are essentially nonadiabatic. It implies that the single crossing of the nonadiabatic transition region results in a small transition probability hence electronic coupling V must be sufficiently small. The DSE regime is a consequence of multiple crossings of the nonadiabatic region. A thorough discussion of the physical mechanisms of the friction influence on the criteria for nonadiabaticity was given in Refs. 16,17. The applicability domain of the stochastic approach for the parameters obtained in this paper may be roughly estimated as $V \lesssim k_B T$.[30] Too large electronic coupling were obtained with the double-channel model ($S_I=0$) as shown by Eqs. (27) and (29). In this case, the adiabatic corrections can be considerable. However, much smaller values have been obtained with the multichannel theory ($S_I=2$): $V=0.048-0.093$ eV [Eqs. (28) and (30)]. The effective electronic coupling between vibrational sublevels is even smaller than these values by the square root of the Franck-Condon factor as indicated by Eqs. (12) and (19). Therefore, the short-time discrepancy cannot be ascribed to a nonapplicability of the model.

As noted above, acetonitrile exhibits a non-Markovian polarization relaxation dynamics. The presence of several relaxation components can affect the ion-pair population dynamics especially at short times.[31] This requires further investigation.

The fit to the experimental data at short times could also be improved by taking into account a nonuniform distribution of inter-reactant distances. This is reasonable if D and A form weak complexes with a coupling energy of the order of $k_B T$. In this case, the number of excited donors with a quencher at contact distance is increased, and the electron transfer rate at early time becomes substantially faster.

The influence of the spatial dispersion on the ion-pair accumulation-recombination kinetics is considered in the next section.

D. Influence of the spatial dispersion of diffusion coefficient and dielectric permittivity on the ion-pair dynamics

The encounter diffusion at large separation differs from that at the closest approach distance where the structure of the few first solvent shells should be taken into account. This can be done phenomenologically by assuming that the diffusion coefficient is r dependent and becomes smaller at shorter distances,[32]

$$D(r) = D\left[1 - \frac{1}{2}\exp\left(\frac{\sigma - r}{\sigma_s}\right)\right], \tag{31}$$

where σ_s is the diameter of a solvent molecule, which amounts to 3.62 Å for acetonitrile, and D is the conventional Fick diffusion coefficient at infinite separation. The actual diffusion coefficient at contact distance is predicted to be about twice as small. The probability for the charge recombination of ion pairs born out of the recombination layer is reduced because their penetration into this layer is slower. A similar effect can be obtained in more viscous solutions by decreasing the Fick diffusion coefficient. In such a diffusion-controlled recombination, observed a few times experimentally,[1,33] the rate decreases with increasing viscosity.[34]

If the spatial dependence of $D(r)$ is taken into account, the spatial dispersion of the dielectric constant $\epsilon(r)$, which affects recombination in the opposite direction, should not be ignored. The spatial dependence of the dielectric constant results from the nonlocal screening of the Coulomb potential.[35,36] The simplest model accounting for the absence of screening at short distances is[35]

$$\epsilon(r) = \frac{\epsilon}{1 + (\epsilon/\epsilon_0 - 1)\gamma \exp(-r/\Lambda)}, \tag{32}$$

where $\epsilon_0=2$ is the optical dielectric constant, ϵ is its static value in the continuum, Λ is a fitting parameter, and $\gamma = 2(\Lambda^2/\sigma^2)(\cosh(\sigma/\Lambda)-1)$ is the correction for the excluded volume of finite-size particles. If this effect is included in $U_c(r)$ appearing in Eq. (15), the Coulomb well becomes deeper,

$$U_c(r) = \frac{e^2}{\epsilon(r) r}. \tag{33}$$

This potential is characterized by a sharp feature near contact, which looks like an additional narrow and rather deep well. It originates from the same Coulomb attraction but is not screened by intercalated solvent molecules. The deepening of the Coulomb well accelerates the drift of ions toward the region of maximum recombination rate, and thus this latter process is enhanced. The depth of this well can be adjusted by the independent parameter Λ.

Accounting for the spatial dispersion of both $\epsilon(r)$ and $D(r)$ improves the fitting of the kinetics $P(t)$ in the interval 30 ps$<t<80$ ps (dashed lines in Fig. 5), but at long time scale the ion state population is still underestimated. For a further improvement of the theory, the chemical anisotropy

of the reaction, which makes all the rates angular dependent and affected by the rotational diffusion,[37] should be taken into account.

E. Internal conversion of the excited ion pairs and free ion yield

In the simple scheme shown in Fig. 1, the potential of the excited ion pair is not displaced horizontally relative to that of the ground state. Since these two potentials do not cross, the electron-vibration interactions are actually absent. Thus, the straightforward transformation of electronic energy of the ion pairs into vibrational energy, followed by vibrational relaxation, is totally ignored. In reality, the two potentials are displaced, and internal conversion can efficiently compete with the above-considered mechanism of double electron transfer, namely, charge recombination of the excited ion pair to the neutral products, followed by hot ionization to the ion pair in the ground state [Fig. 2]. If internal conversion dominates, then all ion pairs are deactivated with 100% efficiency and consequently $\alpha^*=1$.

This alternative has been considered using a time constant of internal conversion of $\tau_{ic}=3$ ps.[7] However, this did not bring any significant change. Although this mechanism produces more ion pairs in the ground state, all of them are born in or near the charge recombination layer and thus recombine much faster than they separate. Therefore their contribution to the free ion yield is negligible. It can thus be concluded that the free ion yield is only weakly sensitive to a particular value of α^*.

IV. HOT RECOMBINATION

The results of the fit indicate a significant role of hot transitions in the recombination dynamics. The effect of hot recombination on the formation of ions depends strongly on the quenching channel. Let us start with the electron transfer to the excited ion pair [Fig. 1], which proceeds in the Marcus normal region (at q_1^*) and is followed by downward diffusion to the bottom of the $D^{+*}A^-$ well. Since the most effective sinks at the $q_2^{*(n)}$ points lie in the Marcus inverted region (Fig. 1), the bottom is reached before the crossing points and the subsequent recombination is mainly thermal, that is, it goes "up and down" from this well to the neutral product potentials.

On the contrary, the charge recombination following the forward electron transfer to the ion pair in the ground state D^+A^- [see Fig. 1] is in the Marcus normal region and includes "down-down" hot transition (Fig. 1). Indeed, starting from a crossing point $q_1^{(n)}$, the system moves down to the intersection points $q_2^{(n)}$ and further down to the bottom of the well. Therefore, the ions pair undergoes first a charge recombination to the neutral product at the points $q_2^{(n)}$ and thermalize afterward. In other words, hot recombination at $q_2^{(n)}$ precedes thermalization, taking away a $(1-\alpha)$ fraction of the ion-pair population and leaving only an α fraction that will recombine thermally ("up-down") afterwards.

On the other hand, the neutral product generated by thermal charge recombination of the excited ion pair also experiences a hot ionization at $q_2^{(n)}(n\leqslant 0)$ before reaching the bottom of the DA state. This is the secondary ionization proceeding with efficiency α^* to the ion-pair state D^+A^- [Fig. 2].

The distributions of ionization products were calculated from Eqs. (26) with the parameters obtained from the best fit of the ionization kinetics Eqs. (27) and (28). As mentioned above, excited ion pairs are produced near contact distance, while those in the ground state are produced in a larger amount and larger distance (see Fig. 4). If we neglect the encounter diffusion of the ions during the motion from q_1 to q_2 and from q_2^* to q_2, the fractions of ions reaching equilibrium by the two parallel pathways can then be estimated as $\alpha(r)m(r)$ and $\alpha^*(r)m^*(r)$. The r distributions of these equilibrated ion pairs are shown by the dash-dotted lines in Fig. 4. These distributions are significantly altered and reduced compared to $m(r)$ and $m^*(r)$ because of hot recombination. These changes arise from $\alpha(r)$ and $\alpha^*(r)$ whose values and space dispersions are calculated below.

The value of α for a system subjected to a single crossing during relaxation has been determined in Refs. 23 and 38. However, the present situation is more complex. Indeed, immediately after the transition to the D^+A^- well near $q_1^{(n)}$, the system almost instantaneously reaches the lowest vibrational level $(n=0)$ because of the ultrafast intramolecular vibrational redistribution and crosses a number of vibrational sublevels of DA while moving toward the bottom of the D^+A^- well (Fig. 1). If these vibrations participate in the charge recombination, i.e., are being Franck-Condon active, the survival probability of the ion pair reduces upon each crossing. Similarly, hot transitions reduce by a factor $1-\alpha^*$ the survival probability of neutral product, which moves down from $q_2^{*(n)}$ toward the bottom of the DA well and crosses several vibrational sublevels of the D^+A^- state.

Following Ref. 26, we consider a sequence of hot electronic transitions to the sublevels $U_{DA}^{(n)}$. The probability of a transition generating n vibrational quanta W_{2n} can be calculated using the method developed in Ref. 23 In the present notation it is given by

$$W_{2n}=\frac{2\pi V_{Rn}^2(r)}{|A_{1n}|}\left[1+2\pi V_{Rn}^2(r)\left(\frac{1}{|A_{1n}|}+\frac{1}{|A_{2n}|}\right)\right]^{-1}, \quad (34)$$

where

$$A_{1n}=\frac{2\lambda}{\tau_L}\frac{\partial U_{D^+A^-}^{(n)}}{\partial q}\bigg|_{q=q_2^{(n)}}=\frac{q_2^{(n)}-2\lambda}{\tau_L},$$
$$A_{2n}=\frac{2\lambda}{\tau_L}\frac{\partial U_{DA}^{(n)}}{\partial q}\bigg|_{q=q_2^{(n)}}=\frac{q_2^{(n)}}{\tau_L} \quad (35)$$

are the slopes of the potential intersecting at $q_2^{(n)}$. Only those points, which are to the right of $q_1^{(0)}$ and whose number is $n_{\max}$, need to be considered.

If $\hbar\Omega\gg k_BT$, the mutual influence of the nearest crossing points is negligible. Under this condition, the survival

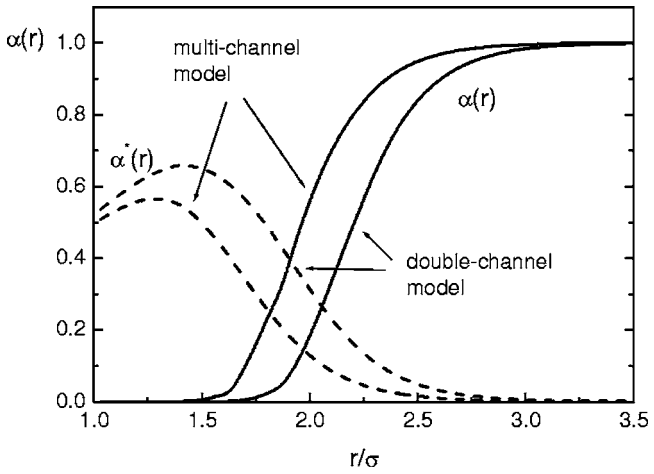

FIG. 6. Fractions of ion pairs having escaped hot recombination to the neutral products α (solid lines) and thermalized fraction of excited ion pairs α^* (dashed lines) as a function of interionic distance r calculated using the double-channel model [Eq. (29)] and the multi-channel model [Eq. (30)].

probability of the ion-pair population is the product of the partial survival probabilities considered as independent events,

$$\alpha(r) = \prod_{n=0}^{n_{\max}} (1 - W_{2n}). \tag{36}$$

The r dependence of α originating from the r dependence of both $V_R(r)$ and $\lambda(r)$ is depicted in Fig. 6.

A similar reasoning can be used to estimate the ground-state ion population generated via the excited-state channel. The value of α^* is

$$\alpha^*(r) = 1 - \prod_{n=0}^{n_{\max}} (1 - W_{1n}), \tag{37}$$

where

$$W_{1n} = \frac{2\pi V_{Rn}^2(r)}{|A_{2n}^*|}\left[1 + 2\pi V_{Rn}^2(r)\left(\frac{1}{|A_{2n}^*|} + \frac{1}{|A_{1n}^*|}\right)\right]^{-1}, \tag{38}$$

$$A_{1n}^* = \frac{q^{*(n)} - 2\lambda}{\tau_L}, \quad A_{2n}^* = \frac{q^{*(n)}}{\tau_L}, \tag{39}$$

where $q^{*(n)} = \lambda - \Delta G_R + n\hbar\Omega$, and $n_{\max}$ is determined from the condition $q^{*(n)} = 2\lambda$. The difference between $\alpha^*(r)$ and $\alpha(r)$ shown in Fig. 6 is most pronounced at large separation where $\alpha^* \to 0$, because hot ionization is switched off, and $\alpha \to 1$, because hot recombination is no longer efficient. Because of the hot transfer processes, the population of thermalized ion pairs is significantly reduced compared to those of their primary generated precursors.

The calculated $\alpha(r)$ and $\alpha^*(r)$ dependencies, along with the initial r distribution of ion pairs $m(r)$ and $m^*(r)$ (Fig. 4), allow the efficiency of hot transitions in both channels to be estimated. Introducing the efficiencies of ion-pair production through the ground and excited channels,

$$P_0 = c \int m(r) d^3 r, \tag{40a}$$

$$P_0^* = c \int m^*(r) d^3 r, \tag{40b}$$

the amounts of thermalized pairs P_{th} and P_{th}^* participating in the subsequent thermal recombination are then calculated as

$$P_{\text{th}} = c \int \alpha(r) m(r) d^3 r, \tag{41a}$$

$$P_{\text{th}}^* = c \int \alpha^*(r) m^*(r) d^3 r. \tag{41b}$$

These parameters, calculated for the double-channel model, are

$$P_0 = 0.89, \quad P_0^* = 0.10, \quad P_{\text{th}} = 0.08, \quad P_{\text{th}}^* = 0.04, \tag{42}$$

and those for the multichannel model are

$$P_0 = 0.96, \quad P_0^* = 0.03, \quad P_{\text{th}} = 0.08, \quad P_{\text{th}}^* = 0.02. \tag{43}$$

Because of the hot transfer, the total amount of thermalized pairs $P_{\text{th}} + P_{\text{th}}^*$ is equal to only 10%–12% of that of the initially generated pairs, $P_0 + P_0^*$. Therefore, for the system considered here, about 90% of the initially created radical ion pairs undergo hot transitions, 4% of them dissociate into free ions, and only 6% recombine through thermal channels.

V. CONCLUSIONS

This is, to our knowledge, the first relatively successful fit of a backward electron transfer kinetics which takes into account the hot recombination of photogenerated ion pairs. The information obtained earlier from the best fit of the forward electron transfer with the same system has been used.[4] This study indicates the presence of two parallel channels of ionization, to the ground and excited states of ion pairs, whose products are located rather far and close to the contact, respectively. Since the backward transfer occurs essentially near contact, the closely spaced excited ion pairs disappear almost completely upon geminate recombination while those in the ground state have a high probability to escape it and thus provide the main contribution into the free ion yield.

The hot recombination of ion pairs is a decisive factor. It is shown that, in the present system, the vast majority of ion pairs have recombined through the hot channel before they are equilibrated and start to recombine with the usual thermal rates. Almost 90% of the ion pairs recombine before equilibrium is reached and the subsequent thermal recombination is accelerated by their encounter diffusion. As a result, no more than 6% of their initial population are finally separated (at $c = 0.32\ M$). Such a surprisingly fast back electron transfer proceeding through the hot channel was also detected in Ru(II)–Co(III) mixed-valence complexes in butyronitrile.[39] In this case as well, less than 50% of the ion pairs generated by the excitation of the metal-to-metal charge-transfer band avoid this recombination and reach equilibrium. These examples show that the study of any system should start from

the inspection of the energy scheme as presented in Fig. 1. This has to be done to find out whether the quenching product has to pass a crossing point (like q_2) on its way to the bottom of the well. If this is the case, one should care not only for thermal but first of all for the hot transfer as a dominant factor in the charge recombination.

Since hot transitions cannot be discussed in terms of rate constant, their appropriate description has called for an extension of existing theories of electron transfer quenching in solutions to explicitly account for reaction coordinate dynamics. In the theory presented here, both the chemical dynamics and the mutual spatial diffusion of the reactants have been taken into account. It should be noted that the spatial motion of the reactants was not considered in previous investigations of hot transitions.[5,6,20–23] In particular, in Ref. 21 the average lifetime of the immobile ion pairs subjected to hot and thermal recombination was calculated. On the contrary, we have considered here the competition between the recombination of thermalized ion pairs and their diffusional separation.

A second new element of the present investigation is connected to the fact that both the ionization and recombination of the Pe-TCNE pairs are considerably affected by the introduction of a high-frequency quantum mode. With such a mode, many term crossings with different values of the vibrational quantum number are available for hot transition. Therefore, the hot recombination efficiency is greatly enhanced. As a result, only the pairs created with a relatively large inter-ionic distance have a finite probability to avoid hot recombination. This allows the unusually small free ion yield of this donor-acceptor pair to be explained.

ACKNOWLEDGMENT

Two of the authors (S.V.F. and A.I.I.) acknowledge the Russian Foundation for Basic Researches for support (Grant No. 05-03-32680).

APPENDIX: SIMULATION METHOD

In the numerical simulations, the Brownian simulation method in the form proposed before in Refs. 38 and 40 was used. Here we outline some features of the program implementation specific to the model considered. The software is available on the web (http://physics.volsu.ru/feskov).

The first step in the simulations is the time propagation of an ensemble of N ($N=10^6-10^7$) Brownian quasiparticles representing the initial distribution of the excited donor-acceptor pairs in extended coordinate space according to the diffusion equations [(8) and (14)] and the reflective boundary conditions at contact radius (21). The important points of the algorithm are as follows.

(1) The initial distribution of quasiparticles obeys Eq. (22).
(2) The unreactive Brownian trajectory of quasiparticle is a Markovian random process in $\{r,q\}$ space.
(3) The electronic transitions in donor-acceptor pairs are modeled by hops of quasiparticles between the potential surfaces (1) at the crossing points $q_i^{(n)}$, $q_i^{*(n)}$ $(i=1,2)$.
(4) The internal conversion of the excited ion pairs is accounted for as an irreversible decay $D^{*+}A^- \rightarrow D^+A^-$ with the characteristic time constant τ_{ic}.

An unreactive trajectory of the kth quasiparticle is calculated as a set of coordinates $\{r_k^{(i)}, q_k^{(i)}\}$ at consecutive time intervals Δt_i. Using well-known Green's functions for the diffusion operators $\hat{\mathbf{D}}$ and $\hat{\mathbf{L}}$ as the probability distributions of random walks at r and q subspaces, one obtains the following simulation rules:

$$q_k^{(i)} = q_k^{(i-1)} e^{-\Delta t_i/\tau_L} + X_i \sqrt{2\lambda(r_k^{(i-1)}) k_B T (1 - e^{-2\Delta t_i/\tau_L})},$$

$$r_k^{(i)} = r_k^{(i-1)} + Y_i \sqrt{2D(r_k^{(i-1)})\Delta t_i} + \frac{2}{r_k^{(i-1)}} D(r_k^{(i-1)})\Delta t_i,$$

for trajectory on the neutral state surface, and

$$q_k^{(i)} = 2\lambda(r_k^{(i-1)}) + (q_k^{(i-1)} - 2\lambda(r_k^{(i-1)})) e^{-\Delta t_i/\tau_L} + X_i \sqrt{2\lambda(r_k^{(i-1)}) k_B T (1 - e^{-2\Delta t_i/\tau_L})},$$

$$r_k^{(i)} = r_k^{(i-1)} + Y_i \sqrt{2D(r_k^{(i-1)})\Delta t_i} + \left(2 - \frac{r_c}{r_k^{(i-1)}}\right) \frac{1}{r_k^{(i-1)}} D(r_k^{(i-1)})\Delta t_i,$$

for that on the ion state surface. Here X_i and Y_i are the Gaussian random numbers with zero mean value and unit dispersion. The above equations are exact for unreactive diffusion along q and are approximate for the spatial diffusion along r, valid for small-time steps.

Each particle is assumed to occupy the volume $\Delta\Gamma$ in the configuration space $\{r,q\}$. This quantity appears naturally when one relates the initial normalized probability distribution function [Eq. (22)] and the finite number N of Brownian quasiparticles. Since the diffusion along r results in an alteration of $\Delta\Gamma$, an additional weight factor $v_k^{(i)}$ is introduced and calculated at each time step as follows:

$$v_k^{(i)} = v_k^{(i-1)} \left(\frac{r_k^{(i-1)}}{r_k^{(i)}}\right)^2, \quad (v_k^{(0)} = 1). \tag{A1}$$

This guarantees the conservation of the distribution function normalization in the absence of reactions

$$\sum_k 4\pi (r_k^{(i)})^2 \Delta\Gamma_k^{(i)} = \Delta\Gamma \sum_k 4\pi (r^{(i)})^2 v_k^{(i)} = \text{const}. \tag{A2}$$

The surface-hopping algorithm[38,41] is applied to simulate electronic transitions between the diabatic surfaces at the crossing points $q_i(r)$. The probability of survival at the same surface is

$$p_k^{(i)} = \exp\left(-\frac{2\pi V_{\text{el}}^2(r_k^{(i-1)})\Delta t_i}{\hbar \Delta U_k^{(i)}}\right), \tag{A3}$$

which is the well-known result of perturbation theory. Here $\Delta U_k^{(i)} = U(r_k^{(i)}, q_k^{(i)}) - U(r_k^{(i-1)}, q_k^{(i-1)})$ and $V_{\text{el}}(r_k^{(i-1)})$ is the corresponding electronic coupling element.

The reaction flux $j(t_i)$ between two free-energy surfaces can be easily calculated through the total configuration volume transferred from one surface to another during the time

interval Δt_i. Since each hop of a quasiparticle generates the elementary flux $\Delta j_k^{(i)} = 4\pi (r_k^{(i)})^2 \Delta\Gamma_k^{(i)} / \Delta t_i$, the total flux is

$$j(t_i) = \sum_k \Delta j_k^{(i)} = \Delta\Gamma / \Delta t_i \sum_k 4\pi (r_k^{(i)})^2 \upsilon_k^{(i)}, \tag{A4}$$

where the summation is taken over particles having transferred between the given surfaces.

The time-dependent survival probabilities of the excited donors $N(t)$ and radical-ion pairs $P(t)$ are then directly determined by the reaction fluxes $j_I(t)$ and $j_R(t)$ for ionization and recombination, respectively. Since the ionization proceeds through two parallel channels the flux $j_I(t)$ is a sum

$$j_I(t) + j_I^*(t) = k_I(t) = \int d^3 r \int dq\ w_I(r,q)\, \nu(r,q,t). \tag{A5}$$

Similarly the recombination fluxes through the ground and excited channels are

$$j_R(t) = \int d^3 r \int dq\ w_R(r,q) \mu(r,q,t), \tag{A6a}$$

$$j_R^*(t) = \int d^3 r \int dq\ w_R^*(r,q) \mu^*(r,q,t). \tag{A6b}$$

Using these quantities, the survival probability of the excited donor state is calculated as

$$N(t) = \exp\left\{ - c \int_0^t j_I(t') dt' - t/\tau_D \right\} \tag{A7}$$

and the kinetics of the ground- and excited-state ion pairs,

$$P(t) = c \int_0^t [j_I(t') N(t') - j_R(t')] dt', \tag{A8}$$

$$P^*(t) = c \int_0^t [j_I^*(t') N(t') - j_R^*(t')] dt'. \tag{A9}$$

The numerical integration in Eqs. (A7) and (A8) is performed by the standard finite-difference methods.

[1] A. I. Burshtein, Adv. Chem. Phys. **114**, 419 (2000).
[2] A. I. Burshtein, J. Lumin. **93**, 229 (2001).
[3] A. A. Zharikov and A. I. Burshtein, J. Chem. Phys. **93**, 5573 (1990).
[4] V. Gladkikh, A. I. Burshtein, G. Angulo, S. Pagès, B. Lang, and E. Vauthey, J. Phys. Chem. A **108**, 6667 (2004).
[5] R. D. Coalson, D. G. Evans, and A. Nitzan, J. Chem. Phys. **101**, 436 (1994).
[6] M. Cho and R. J. Silbey, J. Chem. Phys. **103**, 595 (1995).
[7] S. Pagès, B. Lang, and E. Vauthey, J. Phys. Chem. A **108**, 549 (2004).
[8] L. D. Zusman, Chem. Phys. **49**, 295 (1980).
[9] A. I. Burshtein and B. I. Yakobson, Chem. Phys. **49**, 385 (1980).
[10] A. B. Helman, Chem. Phys. **65**, 271 (1982).
[11] J. N. Onuchic, J. Chem. Phys. **86**, 3925 (1986).
[12] I. Rips and J. Jortner, J. Chem. Phys. **87**, 6513 (1987).
[13] H. Sumi and R. A. Marcus, J. Chem. Phys. **84**, 4272 (1986); **84**, 4894 (1986).
[14] W. Nadler and R. A. Marcus, J. Chem. Phys. **86**, 3906 (1987).
[15] L. D. Zusman, Chem. Phys. **119**, 1988 (51).
[16] A. I. Burshtein and B. I. Yakobson, High Energy Chem. **14**, 211 (1981).
[17] H. Frauenfelder and P. G. Wolynes, Science **229**, 337 (1985).
[18] Y. Georgievski, A. I. Burshtein, and B. M. Chernobrod, J. Chem. Phys. **105**, 3108 (1996).
[19] A. I. Burshtein and A. G. Kofman, Chem. Phys. **40**, 289 (1979).
[20] G. C. Walker, E. Akesson, A. E. Johnson, N. E. Levinger, and P. F. Barbara, J. Phys. Chem. **96**, 3728 (1992).
[21] M. Tachiya and S. Murata, J. Am. Chem. Soc. **116**, 2434 (1994).
[22] J. Najbar, R. C. Dorfman, and M. D. Fayer, J. Chem. Phys. **94**, 1081 (1991).
[23] A. I. Ivanov and V. V. Potovoi, Chem. Phys. **247**, 1999 (245).
[24] A. I. Burshtein, Chem. Phys. Lett. **194**, 247 (1992).
[25] R. C. Dorfman and M. D. Fayer, J. Chem. Phys. **96**, 7410 (1992).
[26] J. Jortner and M. Bixon, J. Chem. Phys. **88**, 167 (1988).
[27] S. A. Passino, Y. Nagasawa, and G. R. Fleming, J. Phys. Chem. A **101**, 725 (1997).
[28] F. Schael and H.-G. Löhmansröben, J. Photochem. Photobiol., A **105**, 317 (1997).
[29] M. G. Kuzmin, I. V. Soboleva, E. V. Dolotova, and D. N. Dogadkin, Photochem. Photobiol. Sci. **2**, 967 (2003).
[30] A. V. Barzykin, P. A. Frantsuzov, K. Seki, and M. Tachiya, Adv. Chem. Phys. **123**, 511 (2002).
[31] O. Nicolet and E. Vauthey, J. Phys. Chem. A **106**, 5553 (2002).
[32] S. F. Swallen, K. Weidemaier, and M. D. Fayer, J. Chem. Phys. **104**, 2976 (1996).
[33] A. I. Burshtein, Adv. Chem. Phys. **129**, 105 (2004).
[34] A. I. Burshtein, J. Chem. Phys. **103**, 7927 (1995).
[35] A. A. Kornyshev and J. Ulstrup, Chem. Phys. Lett. **126**, 74 (1986).
[36] M. A. Vorotyntsev and A. A. Kornyshev, *Electrostatics of a Medium with the Spatial Dispersion* (Nauka, Moscow, 1993).
[37] A. I. Burshtein, I. V. Khudiakov, and B. I. Yakobson, Prog. React. Kinet. **13**, 221 (1984).
[38] S. V. Feskov, A. I. Ivanov, and A. I. Burshtein, J. Chem. Phys. **122**, 124509 (2005).
[39] H. Torieda, K. Nozaki, A. Yoshimura, and T. Ohno, J. Phys. Chem. A **108**, 4819 (2004).
[40] D. J. Bicout and A. Szabo, J. Chem. Phys. **109**, 2325 (1997).
[41] R. G. Fedunov, S. V. Feskov, A. I. Ivanov, O. Nicolet, S. Pagès, and E. Vauthey, J. Chem. Phys. **121**, 3643 (2004).